# Multiple Scattering Analysis within Swarms of CubeSats Devoted to GNSS Reflectometry

Laurent paucot
*ICTEAM*
*Université catholique de Louvain*
Louvain-la-Neuve, Belgium
laurent.paucot@uclouvain.be

Jean Cavillot
*ICTEAM*
*Université catholique de Louvain*
Louvain-la-Neuve, Belgium
jean.cavillot@uclouvain.be

Christophe Craeye
*ICTEAM*
*Université catholique de Louvain*
Louvain-la-Neuve, Belgium
christophe.craeye@uclouvain.be

***Abstract*—The use of CubeSat swarms for GNSS Reflectometry offers a promising approach to improve Earth observation, however it introduces challenges regarding phase synchronization. Indeed, the dynamic positions of the CubeSats induce time-varying distances between satellites. To address this, a distributed antenna array configuration is proposed, and the Method of Moments is employed, accelerated by Macro Basis Functions and multipole expansions, to efficiently model mutual coupling within the swarm. The approach significantly improves computational efficiency while maintaining accuracy, making it suitable for quasi real-time application in digital twins. The analysis provides an order of magnitude of the phase shifts induced by the mutual coupling.**

***Index Terms*—cubesat, GNSS reflectometry, multiple scattering, distributed antenna array, method of moments, macro basis functions, multipole expansion, mutual coupling, phase synchronization, digital twin**

## I. Introduction

Global Navigation Satellite System (GNSS) signals are devoted to provide timing and positioning data. The initial proposal of utilising GNSS reflected signals for Earth observation was put forth by Hall and Cordey in 1988 for scatterometry [1] and by Martin-Neira in 1993 for ocean altimetry [2]. The principal advantage of GNSS reflectometry (GNSS-R) is its bi-static configuration, which enables the deployment of opportunistic platforms dedicated solely to the reception of direct and reflected signals [3]. However, as the signals are constrained to the L band, the ground resolution of GNSS-R systems is directly proportional to the aperture of the receiving antenna. At this frequency, an improvement in resolution would inevitably result in the necessity for excessively large antennas, which in turn would give rise to mechanical and cost-related issues associated with their deployment.

In order to circumvent the necessity for extensive antenna deployment, it has been put forth in [4] that a distributed antenna array be utilized in conjunction with small satellites, most commonly CubeSats, which would be situated in close proximity to one another. The CubeSats are arranged in a 4-arm spiral configuration arranged on concentric ellipses centered on the chief element. The beamforming capability of such a formation enables an improvement in ground resolution. One of the primary challenges associated with distributed radar is the phase synchronization. Indeed, in a traditional phased array, the local oscillator, which is required for baseband demodulation, is distributed to every element through transmission lines. As this is impractical in a CubeSat formation, alternative solutions must be devised. In [4], it has been proposed to implement an architecture wherein a chief satellite is responsible for broadcasting a low-frequency reference tone to the deputies. This reference tone is then up-converted to the L1 band (using a phase-locked loop, for instance) to perform a zero intermediate frequency demodulation.

The issue that has been identified in [4] is that the configuration in question does not remain constant throughout the course of a single orbital cycle. This implies that the distances between deputies and the central chief satellite are not constant over time. Following calibration, the phases must be adjusted in accordance with the displacement of CubeSats, which can be achieved through the pre-computation and measurement of their positions. It is reasonable to anticipate that the reference tone will undergo scattering on the CubeSats themselves, necessitating the incorporation of corrective phase shifts. It is anticipated that a digital twin will be developed to compute all the required correcting factors for beamforming, including those associated with the scattering experienced by the reference tone. Accordingly, a precise and effective methodology is necessary to anticipate the mutual coupling between CubeSats. This is accomplished through the use of the Method of Moments (MoM), which is accelerated by the incorporation of Macro Basis Functions (MBF) [5] and a multipole expansion [6] of the free space Green's function.

This paper is organized as follows. Section II introduces the antenna element that will be considered in the subsequent analysis. Section III provides an overview of the generation and application of MBFs, before introducing the concept of multipole acceleration in Section IV. In Section V, a validation of the proposed method is conducted before an investigation of mutual coupling and a comparison of the timing performance in relation to full-system resolution. This is followed by a conclusion in Section VI.

The present research is part of the Space4ReLaunch project, which is supported by the SPW Economie Emploi Recherche of the Walloon Region, under the grant agreement nr 2210181.

2024 IEEE Conference on Antenna Measurements and Applications (CAMA) | 979-8-3503-8692-9/24/$31.00 ©2024 IEEE | DOI: 10.1109/CAMA62287.2024.10986039

/24/$31.00 ©2024 IEEE

Authorized licensed use limited to: Univ Catholique de Louvain/UCL. Downloaded on June 24,2025 at 22:08:20 UTC from IEEE Xplore. Restrictions apply.

## II. CubeSat Element

In this work, each element of the formation has been assumed to be a 1U CubeSat and simplified to a 10 cm cube surrounded by a $\lambda/4$ monopole antenna, where $\lambda$ is the wavelength. The whole element is assumed to be made of perfect electric conductor. The monopole has a length of 17.3 cm, which corresponds to a quarter wavelength of the 433 MHz frequency of the reference tone. It is assumed that the chief satellite is identical to the deputy satellites. Each element is meshed with 279 basis functions, the majority of which are Rao-Wilston-Glisson functions [7], while rectangular basis functions are used for the monopole. Hybrid basis functions, consisting of half an RWG and half a rectangular one, are used to form the junction with the cube, which may be viewed as a ground plane, and the monopole. A mesh view is shown in Fig. 1.

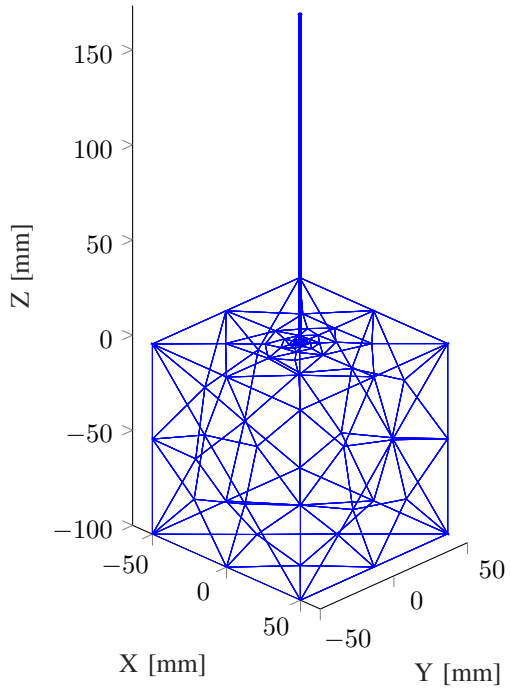



Fig. 1. CubeSat mesh view.

Fig. 2 shows a comparison of the reflection coefficient ($S_{11}$) at the input port, computed on the one hand with the MoM and a delta-gap excitation, on the other hand with CST Microwave Studio®. The results demonstrate a good agreement between MoM and CST simulations, with a good impedance matching at 433 MHz.

## III. Macro Basis Functions

Let us assume an array of $M$ elements, each meshed with $n_e$ elementary basis functions. The MoM system of equations can be expressed as

$$\mathbf{Zx} = \mathbf{v} \tag{1}$$

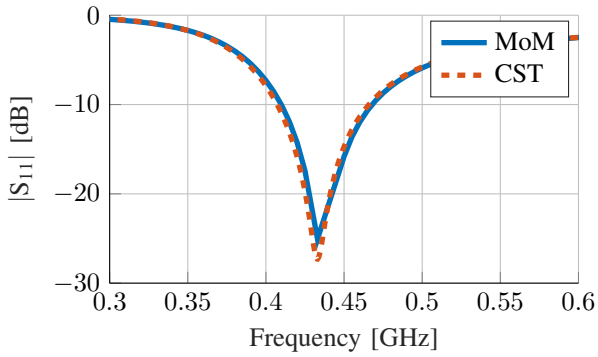



Fig. 2. MoM and CST magnitude of reflection coefficient comparison. Plain blue lines and dashed orange line respectively correspond to MoM and CST solutions.

where $\mathbf{Z}$ is the MoM matrix of impedance [8] composed of $M^2$ $\mathbf{Z_{mn}}$ blocks describing interactions between elements $m$ and $n$, each matrix being of size $n_e \times n_e$. $\mathbf{x}$ is a vector of size $Mn_e$ containing the unknown current coefficients on each basis functions. The excitation vector $\mathbf{v}$ has the same dimension as $\mathbf{x}$. As filling time is proportional to $n_e^2$ and solution time to $n_e^3$, time or memory issues rapidly appear. Therefore, a system reduction can be achieved through the use of a new basis composed of Macro Basis Functions (MBFs) [5]. If Macro Testing Functions (MTFs) are identical to MBFs, impedance matrix and excitation vector respectively reduce to $\mathbf{Z^r_{mn}} = \mathbf{Q^T Z_{mn} Q}$ and $\mathbf{v^r} = \mathbf{Q^T v}$, where $\mathbf{Q}$ is the matrix containing MBFs. Superscripts $^{(\mathrm{r})}$ and $^{(\mathrm{T})}$ stand respectively for *reduced* and *standard transposed*. Full current coefficient vector can be recovered through reduced current vector multiplication by the MBF matrix. Expressions with conjugate transpose instead of standard transpose are also found in the literature. However, it has been shown that accuracy performances are equivalent [9]. Moreover, it allows the maintenance of impedance matrix symmetry and the adherence to electromagnetic reciprocity.

In this work, MBFs have been generated through a multiple scattering approach on the central chief element and the four closest deputies. A primary MBF has been created by computing the current coefficients $\mathbf{x_1^1}$ on the isolated chief CubeSat. The superscript refers to the order of the MBF and the subscript refers to the element. An expression for secondary MBFs is given by $\mathbf{x_{1n}^2} = \mathbf{Z_{nn}^{-1} Z_{n1} x_n^1}$. Tertiary MBFs can be generated with an identical approach and a Singular Value Decomposition (SVD) can be performed to filter out redundant MBFs [10]. This finally results in the construction of the $\mathbf{Q}$ matrix whose column vectors contain the generated MBFs.

## IV. Multipole Expansion

The use of MBFs allows one to accelerate the inversion of the system. However, filling the impedance matrix still remains an issue regarding computational time. Therefore, it has been proposed in [11] and simplified in [12] to make use of a spherical multipole decomposition [6] to derive an

Authorized licensed use limited to: Univ Catholique de Louvain/UCL. Downloaded on June 24,2025 at 22:08:20 UTC from IEEE Xplore. Restrictions apply.

expression allowing to fill in directly the reduced impedance matrix. The interaction between one MBF and one MTF can thus be expressed as

$$I_{pq} = \frac{jk}{(4\pi)^2} \iint \left( j\omega\mu \sum_{n=1}^{n_{ebf}} q_p(n) \vec{F}_n^{\circ}(\hat{u}) \right) \cdot \left( \sum_{n=1}^{n_{ebf}} q_q(n) \vec{F}_n^{\circ}(\hat{u}) \right)^* T(k, \vec{p}_{mn}, \hat{u})\, dU \tag{2}$$

where $j^2 = -1$, $k$ is the wavenumber, $\mu$ is the permittivity of the medium and $q_p$ and $q_q$, being columns of the $\mathbf{Q}$ matrix, are respectively the MBF and MTF coefficients. $\vec{F}_n^{\circ}(\hat{u})$ denotes the far field radiation pattern of elementary basis function $n$ where only components of fields orthogonal to the direction of observation $\hat{u}$ are kept. The operator

$$T(k, \vec{p}_{mn}, \hat{u}) \approx \sum_{l=0}^{L} j^l (2l+1) h_l^{(2)}(k p_{mn}) P_l(\hat{u} \cdot \hat{p}_{mn}) \tag{3}$$

expresses the translation from element $m$ to element $n$ defined by the position vector $\vec{p}_{mn} = p_{mn}\hat{p}_{mn}$. $h_l^{(2)}$ and $P_l$ denote the second kind spherical Hankel function and Legendre polynom of order $l$, respectively.

## V. Performance and Results

### A. Validation

The validation of the MBF-Multipole method is conducted through the computation of self and inter-element scattering parameters $S_{ij}$ at antenna feeders. The parameters are obtained through full system solution as well as MBF reduced system solution, with and without multipole acceleration. The scattering parameters are computed for the initial array configuration represented by the bullets in Fig. 3. This configuration comprises four spiral arms, each comprising seven elements, arranged on concentric ellipsoidal relative orbits to the central chief satellite. The array therefore comprises $M = 29$ elements.

The results are presented in Fig. 4 for the $29^2$ entries of the scattering matrix and five MBFs. The upper figure illustrates the magnitude relative errors of the MBF and MBF-Multipole solution, denoted respectively $\mathbf{x_{MBF}}$ and $\mathbf{x_{MM}}$ in comparison to the MoM full system solution $\mathbf{x}$. Relative errors are computed as

$$\bar{\mathbf{x}}_{\mathbf{MBF/MM}} = 20 \log_{10} \left( \left| \frac{\mathbf{x_{MBF/MM}} - \mathbf{x}}{\mathbf{x_{MBF/MM}}} \right| \right) \tag{4}$$

The bottom figure depicts the absolute phase errors.

As anticipated, multipole acceleration results in a decline in precision due to the use of approximations in the formulation. The aforementioned validation provides insight into the necessity of incorporating a 0.2-degree uncertainty into the phase stability study.

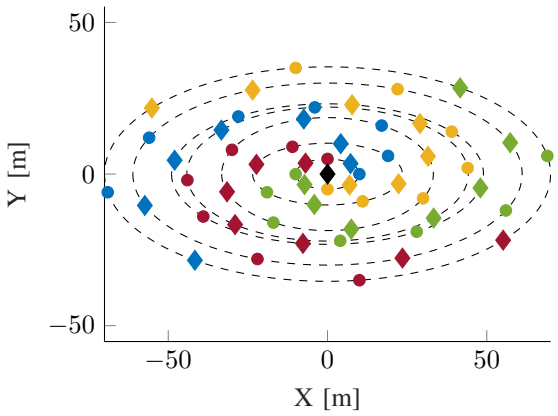



Fig. 3. CubeSat positions. Reference initial configuration is represented with bullets and another arbitrary configuration with diamonds. Colors distinguish the four spiral arms.

### B. Mutual Coupling Analysis

Deputy CubeSats are situated in elliptical relative orbits around the primary satellite. As the distance between one deputy and the central element varies along one orbital cycle, phase shifts induce desynchronization of the reference tone, even if the system has been calibrated in a reference initial configuration. A significant portion of this phase shift can be attributed to the variation in distance, which can be anticipated and corrected through the use of orbital mechanics simulations [13] and in-flight position measurements. A minor contributing factor is inter-platform electromagnetic coupling. It is therefore proposed that a mutual coupling analysis be conducted over the course of half an orbital cycle. A total of 50 simulations are conducted, with one of the illustrative examples presented in Fig. 3 (diamonds). For each CubeSat, the theoretical phase shift and the simulated one, calculated by computing the port scattering parameter phase, are compared. The phase shift differences for a single arbitrary element of the array are illustrated in Fig. 5.

Phase shift errors of up to 2.5 degrees can be observed. It is important to note that in the context of distributed L1-band GNSS-R with a 433 MHz reference tone, the magnitude of the observed errors is increased by a factor of 3.6 given the frequency multiplication. This indicates that internal local oscillators may exhibit phase desynchronization of up to 9 degrees.

### C. Performance

The need to compute mutual coupling for a large number of configurations hinges on the importance of speed performance. Moreover, the long-term objective is to incorporate this computation into a larger digital twin that would operate in quasi real time with the actual swarm. It is therefore of interest to reduce both the number of MBFs employed and the number of integration points involved in the computations of interactions between the MBFs. In this particular context, the scalar product associated with MBF interactions can be

Authorized licensed use limited to: Univ Catholique de Louvain/UCL. Downloaded on June 24,2025 at 22:08:20 UTC from IEEE Xplore. Restrictions apply.

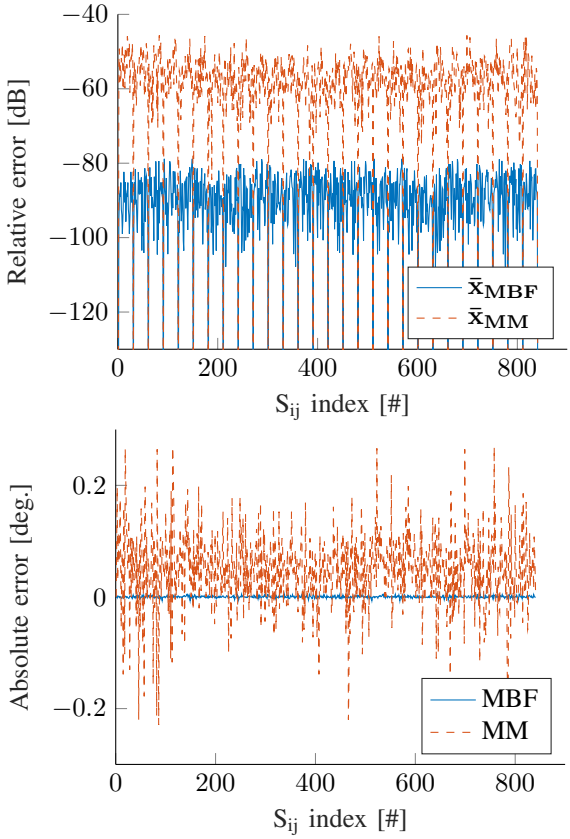



Fig. 4. MBF-Multipole method validation for the reference 29 elements configuration and 5 MBFs. Plain blue lines correspond to the MBF method and dashed orange lines to the MBF-Multipole one. Top: Logarithmic relative error of magnitude scattering parameters. Bottom: Absolute error of phase scattering parameters.

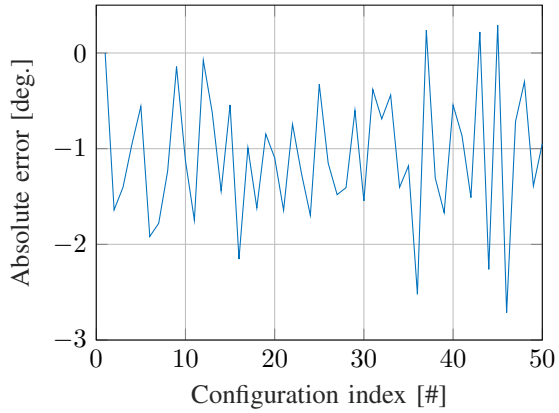



Fig. 5. Phase shift absolute errors due to mutual coupling in the course of half an orbital cycle for an arbitrary element of the array.

precomputed, such that for each novel configuration, the sole term of the integrand to be evaluated is the translation operator. The integration process is accelerated through the implementation of Driscoll weighting for polar angles [14], resulting in the requirement of only 20 points for both polar and azimuth angles. The time required for the computation of the current coefficient on a 29-element configuration is determined through experimentation. The results are presented in Table I. The MBF-Multipole method is performed with the use of five MBFs. The first line corresponds to the time required to fill either the full impedance matrix and excitation vector or their reduced version. In the context of the aforementioned methodology, it is evident that the resolution encompasses solely the system inversion, in the case of the full system method, whilst also encompassing the multiplication of the reduced current coefficient vector by the MBF matrix in the case of the MBF-Multipole method.

TABLE I
CURRENT COEFFICIENT COMPUTATION TIME FOR A 29 ELEMENT CONFIGURATION AND 5 MBFS FOR THE MBF-MULTIPOLE METHOD. TIME DETAIL IS GIVEN FOR IMPEDANCE MATRIX AND EXCITATION VECTOR FILLING SYSTEM RESOLUTION.

| | **Time [s]** | |
|---|---|---|
| | **Full system** | **MBF-Multipole** |
| **Z and v fill** | 203 | 0.09 |
| **Resolution** | 5 | 0.002 |
| **Total** | 208 | 0.092 |

Computation time results show that the MBF-Multipole method runs 2260 times faster than the full system method. It should be noted that the time required to generate the MBFs is not included in the computation time, as this process must be performed only once for all configurations.

## VI. CONCLUSION

This study presented a comprehensive analysis of multiple scattering within CubeSat swarms used for GNSS Reflectometry. By employing the MoM combined with Macro Basis Functions and multipole expansions, significant improvements in computational efficiency were achieved while maintaining accuracy. The proposed MBF-Multipole method allows for rapid evaluation of mutual coupling effects and phase shift errors across various configurations during CubeSat orbital cycles. This method has proven to be multiple order of magnitude times faster than a traditional full system approach, making it highly suitable for real-time applications within digital-twin frameworks. The analysis provided an order of magnitude of the phase shift errors induced by mutual coupling. After frequency multiplication, these errors can induce phase desynchronization of the internal local oscillators up to 9 degrees.

## REFERENCES

[1] C. Hall and R. Cordey, "Multistatic scatterometry," in *Inter. Geosci. Remote Sens. Symp.*, vol. 1, Edinburgh, United Kingdom, Sep. 1988, pp. 561–562.

[2] M. Martin-Neira *et al.*, "A passive reflectometry and interferometry system (paris): Application to ocean altimetry," *ESA journal*, vol. 17, no. 4, pp. 331–355, 1993.

[3] V. U. Zavorotny, S. Gleason, E. Cardellach, and A. Camps, "Tutorial on remote sensing using GNSS bistatic radar of opportunity," *IEEE Geosci. Remote Sens. Mag.*, vol. 2, no. 4, pp. 8–45, Dec. 2014.

Authorized licensed use limited to: Univ Catholique de Louvain/UCL. Downloaded on June 24,2025 at 22:08:20 UTC from IEEE Xplore. Restrictions apply.

[4] L. Paucot, E. Hubin, M. Drouguet, V. Kudriashov, J. Thoemel, and C. Craeye, "CubeSat formation antenna array synchronization for GNSS-R," in *18th Europ. Conf. Antennas Propag. (EuCAP)*, Glasgow, United Kingdom, Mar. 2024, pp. 1–5.
[5] E. Suter and J. R. Mosig, "A subdomain multilevel approach for the efficient mom analysis of large planar antennas," *Microw. Opt. Technol. Lett.*, vol. 26, no. 4, pp. 270–277, Aug. 2000.
[6] R. Coifman, V. Rokhlin, and S. Wandzura, "The fast multipole method for the wave equation: a pedestrian prescription," *IEEE Antennas Propag. Mag.*, vol. 35, no. 3, pp. 7–12, Jun. 1993.
[7] S. Rao, D. Wilton, and A. Glisson, "Electromagnetic scattering by surfaces of arbitrary shape," *IEEE Trans. Antennas Propag.*, vol. 30, no. 3, pp. 409–418, May 1982.
[8] R. F. Harrington, *Field Computation by Moment Methods*. Piscataway, New Jersey: IEEE Press, 2015.
[9] D. Gonzalez-Ovejero, F. Mesa, and C. Craeye, "Accelerated macro basis functions analysis of finite printed antenna arrays through 2d and 3d multipole expansions," *IEEE Trans. Antennas Propag.*, vol. 61, no. 2, pp. 707–717, Feb. 2013.
[10] E. Lucente, A. Monorchio, and R. Mittra, "An iteration-free mom approach based on excitation independent characteristic basis functions for solving large multiscale electromagnetic scattering problems," *IEEE Trans. Antennas Propag.*, vol. 56, no. 4, pp. 999–1007, Apr. 2008.
[11] C. Craeye, "A fast impedance and pattern computation scheme for finite antenna arrays," *IEEE Trans. Antennas Propag.*, vol. 54, no. 10, pp. 3030–3034, Oct. 2006.
[12] C. Craeye, T. Gilles, and X. Dardenne, "Efficient full-wave characterization of arrays of antennas embedded in finite dielectric volumes," *Radio Sci.*, vol. 44, no. 1, Feb. 2009.
[13] E. Hubin, "Cubsats's study in formation for earth observation," 2023. [Online]. Available: http://hdl.handle.net/2078.1/thesis:43312
[14] J. Driscoll and D. Healy, "Computing fourier transforms and convolutions on the 2-sphere," *Adv. Appl. Math.*, vol. 15, no. 2, pp. 202–250, Jun. 1994.

Authorized licensed use limited to: Univ Catholique de Louvain/UCL. Downloaded on June 24,2025 at 22:08:20 UTC from IEEE Xplore. Restrictions apply.